2012 International Conference on Image, Vision and Computing (ICIVC 2012)
IPCSIT vol. 50 (2012) © (2012) IACSIT Press, Singapore
DOI: 10.7763/IPCSIT.2012.V50.8

The Quantitative Bone Microarchitectural Based Computer Aided Analysis for Osteoporosis Detection Using Digital Hip Radiograph

V. Sapthagirivasan [1 +], M. Anburajan [2] and Venkatesh Mahadevan [3]

[1, 2] SRM University, Kattankulathur, Chennai, India

[3] Swine Burne University of Technology, Australia

Abstract. The quality of life can be improved and risk of fractures would be effectively reduced, by the proper initial diagnosis of the osteoporotic abnormality. The identification of low bone mineral density (BMD) or the onset of osteoporosis can be performed by means of detecting the extracted trabecular features from digital hip radiographs. The objective of our study was to apply a gradient based image processing technique from simple X-ray in order to measure trabecular structure for osteoporosis evaluation and its associated fracture risks. Fifty South Indian women were chosen for whom DXA (DPX Prodigy, GE-Lunar Corp., USA) as well X-ray (Multiphos, Siemens, Germany) measurements were acquired from the right proximal region. For the digital X-rays acquired, gradient based texture image analysis was performed; multiple linear regression models which is the combination of age and gradient texture has outputted predicted BMD in order to distinguish normal group from osteoporotic one. None of the textural (run-length) variables have exhibited significant correlation with DXA variables in case of original radiographs. Whereas, the gradient based method has demonstrated significant co-relational emphasis with textural (HGRE - High gray-level run emphasis) parameter with Neck and Ward's region of DXA BMDs. Also, the regression model has displayed significant co-relational impact with all anatomical sites of DXA BMDs. Our results emphasize that the predicted BMD extracted from digital hip X-ray image would be useful as a low cost screening tool for osteoporosis diagnosis and its associated fracture risks.

Keywords: gradient approach, texture analysis, trabecular analysis, run-length, femur X-ray, DXA.

1. Introduction

The developing as well as the developed countries, are both witnessing the rampant increase in ageing population. The disability, dependence as well as associated economic and social problems, those are caused by osteoporosis is being referred by elderly population and public health workers. Unless and otherwise fractures happen, the onset of osteoporotic prediction would be unknown. Hence, the other name for osteoporosis is 'silent epidemic'. The devices such as duel energy x-ray absorptiometry (DXA) have been utilized for estimating the presence of osteoporosis so that the epidemic can be properly controlled. The DXA, in a way has helped to improve the quality of life. The bone mineral content evaluation would go a long way in helping osteoporotic prediction [1].

India has not been well equipped with the facilitative considerations such as QCT [2], single photon absorptiometry [3] and DXA. The role of bone structure has been considered as the prime factor in bone quality determination in terms of bone mineral density (BMD) [4-5]; clinical technique such as bone ultrasonic assessment are unclear regarding the contributions being provided to the measured variables and have been believed to depict structural information only [6]. These facilities exist in selected centers only. This sophisticated investigation still needs sufficient variation with respect to general population. The X-ray image analysis has been earlier, utilized for bone structure measurement [7-15]. By 1970 itself, Singh et al [16] reported an index for assessing degree of osteoporosis by witnessing changes in the trabecular pattern of

+ Corresponding author. Tel.: +91-44-2249 2882; fax: +91-44-2249 1777.
E-mail address: sapthagiri.ece@gmail.com.

proximal femur and a significant correlation was evidenced between radiological and histological parameters. Even though the conventional radiography has high accessibility, it is of utmost necessity to innovate the amicability of the mechanical competence of the bones. Radiography can be utilized to process, both bone geometry as well as trabecular structure; the relevant image processing technique would be used to decipher bone density information. The intensity and contrast variations of X-ray image acquisition conditions between images are the main constraints in bone density precise evaluation. Theoretically image local gradients are independent with respect to intensity and contrast level and thus might provide an opportunity to solve the problem. The trabecular bone analysis adopted the gradient method morphological features as reported by Veenland et al [15, 17-18].

The main objective of the proposed study was to implement a gradient based image processing method from simple radiograph for the trabecular structure measurement to evaluate osteoporosis and its allied risks of fracture.

2. Materials and Methods

2.1. Subjects

The present study consisted of fifty pre- and post- menopausal South Indian women residing in Chennai, India (latitude 13.08 °). These participants were selected, when they arrived for their BMD measurements, as part of their routine health checkup. All the participants expressed their voluntary willingness in order to conduct other tests and they also signed the prescribed form as part of informed consent. The health care ethics department of SRM University approved the study protocol after careful examination. The participants with known complaints of hepatic, renal, dermatological disorders, Paget's diseases, Rheumatoid arthritis or chronic renal dysfunction, endocrinal abnormalities that could impact thyroid, parathyroid and adrenal glands affectively, alcoholism, or receiving medication which would adversely impact the bone health were expelled from the study. The clinical data involving fracture history, anthropometric as well as demographic data were confirmed and an elaborate physical examination was conducted. The ratio of weight in kilo gram to the square of height in meters was used to calculate Body mass index (BMI).

2.2. Bone mineral density

The standard protocol was followed in acquiring BMD at the different sites of right proximal femur (Neck, Ward's region, trochanter, shaft and total femur) by DPX Prodigy (DXA Scanner, GE-Lunar Corp., USA). The WHO cut-offs for osteoporosis classification was used to categorize normal (T-score ≥ -1), osteopenia (T-score between -1 and -2.5) and osteoporosis (T-score ≤ -2.5) at total femoral BMD. The manufacturer's recommendations were carefully followed to manifest quality control procedures. The manufacturer contributed a phantom in order to regulate instrument variation and the mean coefficient of variation was <0.5%.

2.3. Diagnostic imaging

The digital x-ray machine (Multiphos, Siemens, Germany) with tube voltage of 45 to 80 kV, 2 mA exposure conditions was used to acquire the digital radiograph of right hip in all studied South Indian women. While acquiring the image, the due care was taken to see that, there was 15^0 internal rotation of femur region. There was direct digitization of the radiographs with 12 bit (12 bits per pixel) depth and DICOM analytical format was used for further analysis. After acquiring DXA measurements, the digital radiographs were taken within the prescribed period of 3 days.

2.4. Quantitative analysis

Due to the fact that, the partial derivatives are not rotation invariant, the gradient calculation was done twice, both in horizontal and vertical direction. As the gradients are less prone to lighting and focuses, the matching error can be minimized. The initial reconstruction of the gradient based gray level image was done by the multiplication of original image with the gradient matrix calculated in both the directions.

The distribution of trabecular patterns in standard radiographs of the right hip in pre-defined region of interest (ROI) using the texture analysis was measured. A trained operator was positioned a 128 X 128 pixel ROI at the clinically significant area as displayed in Fig.1 on each right proximal femur pre-processed X-ray

image (Fig. 2) and fed in to the algorithm that has been developed using Matlab 7.0 software programming. In order to speed up the computing time, the 256 gray level images were mapped to 16 gray levels. A run can be incorporated by the consecutive pixels of the same gray value in a given direction [19-20]. In our study, for horizontal (H) and vertical (V) directions, run length variables were thus measured and the mean value was considered for analysis. The run length variables have been detailed elsewhere and are comprised of [19-20].

- SRE (HSRE and VSRE): the occurrence of short-runs controls the long-run emphasis (horizontal and vertical) and is presumed to be ample for coarse structural textures.
- LRE (HLRE and VLRE): the occurrence of long-run controls long-run emphasis (horizontal and vertical) and is presumed to be large for coarse structural textures.
- GLN (HGLN and VGLN): the similarities of gray-level values throughout the image were measured by the gray-level non-uniformity (horizontal and vertical). In case, the gray-levels are alike throughout the image, the GLN is expected to be small.
- RLN (HRLN and VRLN): the similarities of the lengths of the runs throughout the image were measured by run-length non-uniformity (horizontal and vertical). If the run-lengths are alike throughout the image, the RLN is expected to be small.
- RP (HRP and VRP): the homogeneity and distribution of runs of image in a specific direction were measured by run percentage (horizontal and vertical). For an image with a homogeneous texture, the RP is expected to be large.
- LGRE (HLGRE and VLGRE): the occurence of runs with a low gray-level (black, deep gray) controls the low gray-level run emphasis (horizontal and vertical).
- HGRE (HHGRE and VHGRE): the occurrence of runs with a high gray-level (white, light gray) controls the high gray-level run emphasis (horizontal and vertical).

The semi-empirical formula for the purpose of predicting femoral-neck BMD (PFN-BMD) has been deduced on the basis of multiple linear regression models as follows:

$$Y = 0.942167 + \left(\frac{0.69819}{2^n - 1} \right) * X_1 \; ? \; 0.0061605 * X_2 \qquad (1)$$

Where,

Y – Predicted femoral neck BMD (PFN-BMD) in g/cm^2, X_1 – HGRE in gray levels and X_2 – Age of the subject in years, n – Number of bits per pixel per gray level.

2.5. Statistical tests

The SPSS software package version 17.0 (SPSS Inc., Chicago, USA) and Micro-soft Excel version 2007 (MS-Office package, Microsoft Inc., Redmond, USA) had been used to analyze the data. The presentation of data was in terms of either mean ± SD or number (%) unless specified. In order to compare and calculate the mean BMD values for all categories, the un-paired Student's t-test was administered. The Pearson's correlation and linear regression testes were adopted in order to evaluate the strength of relationship between BMD and other variables. A p value of <0.05 was claimed to display statistical significance.

3. Results

The total studied population of 50 South Indian women was divided into normal, osteopenia as well as osteoporosis groups based on the total femoral T-score. Out of the total studied population; normal (n=23, age= 44.0 ± 11.0), osteopenia (n=17, age=47.7 ± 11.6) as well as osteoporosis (n=10, age=64 ± 11.4) categories have been carefully analyzed and results are interpreted as follows:

Table 1 detail the Pearson's co-relational aspects of anthropometric, demographic as well as BMD features against run-length features of plain radiographs. Age and Ward's BMD have displayed the significant correlation at the level of p< 0.05 with HGRE. Height has shown co-relational significance with

SRE, RP as well as RLN at the level of p< 0.05. Weight, BMI, right femoral: Neck, trochanter, shaft and total BMDs displayed no co-relational impact with any of the run-length features of plain radiograph.

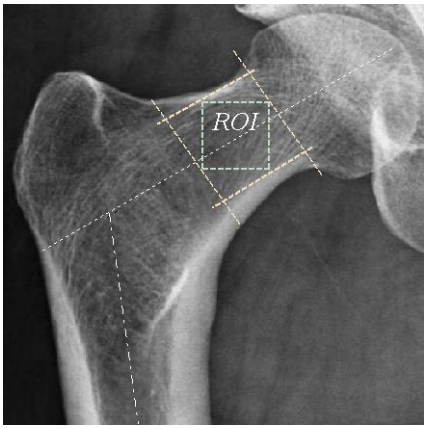

Fig. 1: plain radiograph of right hip with marked ROI

Table. 1: Pearson's correlation of run-length features of plain radiograph vs. demographic, anthropometric and BMDs features

Variables / Image features	SRE	LRE	GLN	RP	RLN	LGRE	HGRE
Age (year)	0.054	-0.002	0.145	0.060	-0.001	0.149	-0.340*
Height (cm)	0.313*	-0.114	0.219	0.344*	0.341*	-0.105	0.096
Weight (kg)	0.193	0.004	0.055	0.140	0.163	0.194	-0.058
BMI (kg/m^2)	0.070	0.054	-0.048	-0.010	0.018	0.254	-0.101
Right femoral BMDs (g/cm^2)							
Neck	0.005	0.019	-0.171	-0.027	0.009	-0.094	0.253
Ward's	0.026	-0.019	-0.131	0.000	0.014	-0.142	0.296*
Trochanter	-0.047	-0.051	-0.172	-0.060	-0.058	-0.006	0.180
Shaft	-0.005	0.005	-0.114	-0.041	-0.020	0.043	0.124
Total	-0.046	-0.004	-0.189	-0.074	-0.059	0.014	0.158

*. Correlation is significant at the 0.05 level (2-tailed).

Following is the description of demographic, anthropometric as well as BMD feature's Pearson co-relational analysis against run-length features of gradient image which has been displayed in Table 2. Age, neck as well as Ward's BMD exhibited co-relational significance at the level of p<0.05, p<0.01 and p<0.01 respectively with HGRE. Height exhibited co-relational impact at the level of p<0.05 with SRE and RP. As per the multiple linear regression analytical framework, in the event of the combination of age and HGRE, age; neck, ward, trochanter, shaft, total BMD displayed the impact of correlation at the level of p<0.01; height at p<0.05, as informed in Table 2.

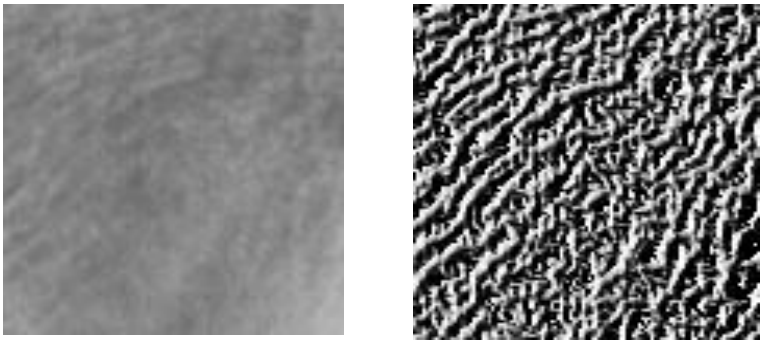

Fig. 2: (a) original ROI, (b) gradient of (a)

Table. 2: Pearson's correlation of run-length features of gradient image vs. demographic, anthropometric and BMDs features

Variables / Image features	SRE	LRE	GLN	RP	RLN	LGRE	HGRE	Regression (Age + HGRE)
Age (year)	0.276	-0.025	0.254	0.143	-0.081	0.159	-0.335*	-0.892**
Height (cm)	0.322*	-0.141	0.160	0.353*	0.208	-0.171	0.183	0.320*
Weight (kg)	-0.002	0.040	0.002	0.013	-0.099	0.031	0.122	0.181
BMI (kg/m^2)	-0.165	0.109	-0.083	-0.160	-0.205	0.104	0.060	0.056
Right femoral BMDs (g/cm^2)								
Neck	-0.191	0.048	-0.220	-0.101	0.054	-0.196	0.354**	0.654**
Ward's	-0.150	0.005	-0.178	-0.058	0.046	-0.266	0.395**	0.672**
Trochanter	-0.198	-0.015	-0.185	-0.113	-0.016	-0.159	0.276	0.560**
Shaft	-0.167	0.038	-0.133	-0.109	-0.047	-0.074	0.204	0.472**
Total	-0.223	0.035	-0.210	-0.147	-0.056	-0.126	0.263	0.572**

*. Correlation is significant at the 0.05 level (2-tailed); **. Correlation is significant at the 0.01 level (2-tailed).

The description of the following facts and figures, which is a analytical background based on total femur BMD categorization of normal, osteopenia and osteoporosis samples has been communicated in Table 3. Age has displayed significance at the level of $p<0.001$, when osteopenic and osteoporosis as well as normal and osteoporosis groups were compared. Weight has demonstrated significant impact at the level of $p<0.05$ and $p<0.001$, when the comparison was done between osteopenic and osteoporosis as well as normal and osteoporosis group respectively. Similarly, BMI has demonstrated significant impact at the level of $p<0.05$ and $p<0.01$, when the comparison was done between osteopenic and osteoporosis as well as normal and osteoporosis group respectively. Predicted femoral neck BMD exhibited the co-relational impact at the level of $p<0.001$, when the comparison was manifested between osteopenic and osteoporosis as well as normal and osteoporosis group.

Table. 3: Analysis based on Total Femur BMD classification of normal, osteopenia and osteoporosis

Variables / Groups	Normal (n=23)	Osteopenia (n=17)	Osteoporosis (n=10)	*p* value [c]
Age (years)	44.0 ±11.0	47.7 ±11.6	64 ±11.4 ***[b]	0.00005
Height (cm)	151.5 ±5.6	148.7 ±4.8	147.7 ±6.9	0.10210
Weight (kg)	58.7 ±9.9	53.5 ±8.8	46.2 ±5.2*[b]	0.00073
BMI (kg/m^2)	25.6 ±4.3	24.1 ±3.8	21.2 ±2.0*[b]	0.00420
Right femoral BMDs (g/cm^2)				
Neck (DXA)	0.978 ±0.13****[a]	0.774 ±0.04	0.629 ±0.09 ****[b]	0.00000
Total (DXA)	1.026 ±0.11****[a]	0.778 ±0.07	0.588 ±0.1****[b]	0.00000
Linear regression model (Age + HGRE of gradient image)				
Predicted-Neck (X-ray)	0.888 ±0.1	0.839 ±0.1	0.739 ±0.09 **[b]	0.00027

[n] Indicates number of subjects in each subgroup; *$p<0.05$; **$p<0.01$; ***$p<0.001$; ****$p<0.000001$

[a] Comparison between normal and osteopenia group; [b] Comparison between osteopenia and osteoporosis group;

[c] Comparison between normal and osteoporosis group

The ROI that has been extracted from plain radiograph as well as the gradient image is displayed in figure 2. The co-relational significant aspects of femoral neck, Ward's, trochanter, shaft and total BMDs against predicted femoral neck BMD that has been extracted from hip X-ray image as shown in figure 3.

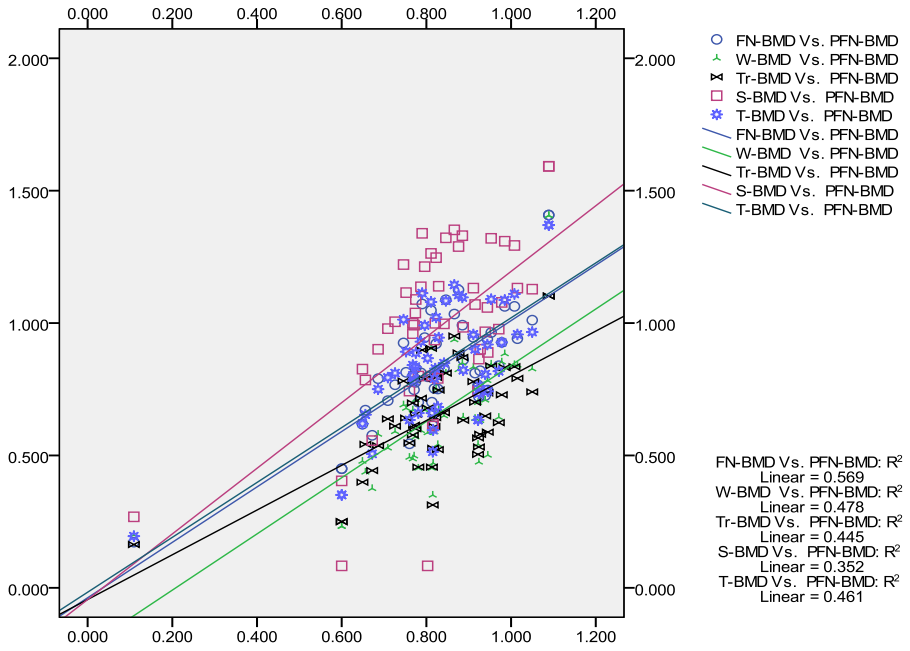

Fig.3 Correlation of PFN-BMD (predicted BMD) extracted from hip x-ray image vs. neck, Ward's, trochanter, shaft and total femur BMDs by central DXA

4. Discussion

Osteoporosis initiates the widening of trabecular separation, by means of trabecular number reduction; reduction in the thickness as well as their connections. These alterations would come out with X-ray attenuation modification and change the texture and density of the image.

In the present study, we have examined the hypothesis that proximal femur trabecular bone variables' features, obtained from digital hip radiograph are able to diagnose osteoporosis and its allied fracture risk. As such, the radiographic methods are widely accessible throughout the globe and they will be suitable for the utilization of trabecular structure identity. So, these radiographs if used for the detection of osteoporosis and its associated fracture risk, it would be a beneficial task, especially in locations, where DXA is not widely accessed.

The event of combination of age and trabecular bone structure facilitates the quantitative features extracted from digital radiographs to have significantly associated with DXA based BMD. Our study claims that a major proportion of the variability in DXA based BMD can be evaluated from radiographs. Many authors have proclaimed in accordance with our present study, that the textural analysis of trabecular bone derived from radiographs would detect osteoporosis patients from control groups [9, 10, 12, 13, 15].

According to our study, the run-length texture features extracted from gradient based radiographs has exhibited significant co-relational impact with DXA BMD obtained from Neck and Ward's region of right femur. Similar study as that of Guggenbuhl et al reported that the X-ray texture analysis could be an appropriate technique for 2-D bone microarchitecture assessment. Next, a positive correlation was evidenced between texture analysis of X-ray image and 3-D bone micro-architecture, which has been measured by micro computed tomography [14]. Chappard et al reported the significant co-relational impact of BMD with textural features in site matched locations and also emphasized the use of plain radiographs in place of BMD measurements [13]. Pulkkinen et al utilized the numerous radiograph based geometrical and trabecular texture variables in combination model in order to distinguish between fracture patients and control groups [21]. On the contrary, an earlier study has displayed a poor value of texture features, when implied on plain lumbar spine X-ray films [22]. Similarly, in current study as detailed in Table 1, the texture variables extracted from plain radiograph have demonstrated poor value of co-relational significance vs. DXA BMDs. However, in our gradient based approach, the combination regression model which is the combination of age and run-length (HGRE) feature has demonstrated high co-relational impact with right

femur region BMDs measured at all anatomical sites (Table 2); also when the comparison need to be made (in combination model) between normal and osteoporosis group, a high significance of $p<0.001$ has been evidenced by predicted femoral neck BMD (Table 3).

5. Conclusion

The conclusion of the study is that, a novel hypothesis has been constructively deduced by the consideration of extracted proximal femur trabecular bone features. The predicted neck BMD extracted from X-ray image which has been the outcome of multiple linear regression models, the combination of gradient texture feature and age has been outputted in order to sort out normal group from osteoporotic group and henceforth would be useful in osteoporosis diagnosis and its associated fracture risks in the proposed low cost environment.

6. Acknowledgment

The authors sincerely attribute their gratitude to SRM hospital staffs as well as Mr. Kishore Mohan KB, fulltime research scholar, Department of Biomedical Engineering SRM University. All related expenditure pertaining to research work has been managed by first author. The authors declare no conflict of interest.

7. References

[1] Osteoporosis facts and statistics: [online] http://www.iofbonehealth.com/bonehealth/facts-and-statistics-0

[2] C. E. Cann, H. K. Genant, F. O. Kolb, and G. Ettinger. Quantitative computed tomography for the prediction of vertebral fracture risk. *Bone*, **6**:1–7, 1986

[3] J. R. Cameron, R. B. Mazess, and M. S. Sorenson. Precision and accuracy of bone mineral determination by direct photon absorptiometry. *Invest. Radiol.* **3**:141–150, 1968

[4] L. Mosekilde, L. Mosekilde, and C. C. Danielsson. Biomechanical competence of vertebral trabecular bone in relation to ash density and age in normal individuals. *Bone*, **8**:79–85, 1987

[5] L. Mosekilde. Age related changes in vertebral bone architecture assessed by a new method. *Bone*, **9**:247–250, 1988

[6] C. Langton. The role of ultrasound in the assessment of osteoporosis. *Clin. Rheumatol*, **13**(S1):13–17, 1994

[7] C. Chappard, B. Brunet-Imbault, G. Lemineur, B. Girardeau, A. Basillais, R. Harba, C. L. Benhamou. Anisotropy changes in post-menopausal osteoporosis: characterization by a new index applied to trabecular bone radiographic images. *Osteoporos Int*. **16**:1193–1202, 2005

[8] C. L. Benhamou, S. Poupon, E. Lespessailles, S. Loiseau, R. Jennane, V. Siroux, W. Ohley, L. Pothuaud. Fractal analysis of radiographic trabecular bone texture and bone mineral density: two complementary parameters related to osteoporotic fractures. *J Bone Miner Res.* **16**:697–704, 2001

[9] T. J. Vokes, M. L. Giger, M. R. Chinander, T. G. Karrison, M. J. Favus, L. B. Dixon. Radiographic texture analysis of densitometer generated calcaneus images differentiates postmenopausal women with and without fractures. *Osteoporos Int.* **17**:1472–1482, 2006

[10] L. Pothuaud, E. Lespessailles, R. Harba, R. Jennane, V. Royant, E. Eynard, C. L. Benhamou. Fractal analysis of trabecular bone texture on radiographs: discriminant value in postmenopausal osteoporosis. *Osteoporos Int*. **8**:618–625, 1998

[11] J. S. Gregory, A. Stewart, P. E. Undrill, D. M. Reid, R. M. Aspden. Identification of hip fracture patients from radiographs using Fourier analysis of the trabecular structure: a cross-sectional study. *BMC Med Imaging*. **4**:4, 2004

[12] J. C. Lin, S. Grampp, T. Link, M. Kothari, D. C. Newitt, D. Felsenberg, S. Majumdar. Fractal analysis of proximal femur radiographs: correlation with biomechanical properties and bone mineral density. *Osteoporos Int.* **9**:516–524, 1999

[13] D. Chappard, A. Chennebault, M. Moreau, E. Legrand, M. Audran, M. F. Basle. Texture analysis of X-ray radiographs is a more reliable descriptor of bone loss than mineral content in a rat model of localized disuse induced by the Clostridium botulinum toxin. *Bone.* **28**:72–79, 2001

[14] P. Guggenbuhl, F. Bodic, L. Hamel, M. F. Basle, D. Chappard. Texture analysis of X-ray radiographs of iliac bone is correlated with bone micro-CT. *Osteoporos Int.* **17**:447–454, 2006

[15] J. F. Veenland, J. L. Grashuis, H. Weinans, M. Ding, H. A. Vrooman. Suitability of texture features to assess changes in trabecular bone architecture. *Pattern Recogn Lett.* **23**:395–403, 2002

[16] M. Singh, A. R. Nagrath, P. S. Maini. Changes in trabecular pattern of the upper end of the femur as an index of osteoporosis. *J Bone Joint Surg Am.* **52**:457–467, 1970

[17] J. F. Veenland, T. M. Link, W. Konermann, N. Meier, J. L. Grashuis, E. S. Gelsema. Unraveling the role of structure and density in determining vertebral bone strength. *Calcif Tissue Int.* **61**:474–479, 1997

[18] J. F. Veenland, J. L. Grashuis, E. S. Gelsema. Texture analysis in radiographs: the influence of modulation transfer function and noise on the discriminative ability of texture features. *Med Phys.* **25**:922–936, 1998

[19] M. M. Galloway. Texture analyses using gray level run lengths. *Comput Graph Image Proc*. **4**:172–179, 1975

[20] A. Chu, C. M. Sehgal, J. F. Greenleaf. Use of gray value distribution of run lengths for texture analysis. *Patt Recogn Lett.* **11**:415–419, 1990

[21] P. Pulkkinen, T. Jamsa, E. M. Lochmuller, V. Kuhn, M. T. Nieminen, F. Eckstein. Experimental hip fracture load can be predicted from plain radiography by combined analysis of trabecular bone structure and bone geometry. *Osteoporos Int.* **19**:547–558, 2008

[22] P. Caligiuri, M. L. Giger, M. J. Favus, H. Jia, K. Doi, L. B. Dixon. Computerized radiographic analysis of osteoporosis: preliminary evaluation. *Radiology.* **186**:471–474, 1993